Single-crystal and powder neutron diffraction study of the $Fe_XMn_{1-X}S$ solid solutions

Galina Abramova [a,*], Juerg Schefer [b], Nadir Aliouane [b], Martin Boehm [c], German Petrakovskiy [a], Alexandr Vorotynov [a], Mikhail Gorev [a,e], Asya Bovina [a], Vladimir Sokolov [d]

[a] Kirensky Institute of Physics, Russian Academy of Sciences, Siberian Branch, Krasnoyarsk 660036, Russia
[b] Paul Scherrer Institute, Laboratory for Neutron Scattering (LNS), CH-5232 Villigen PSI, Switzerland
[c] Institut Max von Laue – Paul Langevin, Grenoble Cedex 9, France
[d] Nikolaev Institute of Inorganic Chemistry, Siberian Branch, Russian Academy of Sciences, Novosibirsk 630090, Russia
[e] Institute of Engineering Physics and Radio Electronics, Siberian Federal University, pr. Svobodny 79, Krasnoyarsk 660041, Russia

ARTICLE INFO

ABSTRACT

The α-MnS-based $Fe_XMn_{1-X}S$ ($0 < x < 0.3$) solid solutions are synthesized and shown to be new Mott materials with the rock salt structure. Neutron diffraction data show that the chemical-pressure-induced Neel temperature shift from 150 ($x = 0$) to 200 K ($x = 0.29$) observed in these materials is accompanied by a decrease in the NaCl-type cubic lattice parameters. It is established that at the symmetry transformation in the compositions with $x = 0.25$ and 0.29 the structural transition occurs, which is followed by the magnetic transition. These features make the $Fe_XMn_{1-X}S$ solid solutions interesting for both fundamental study of the interrelation between the magnetic, electrical, and structural properties in MnO-type strongly correlated electron systems and application.

© 2015 Elsevier B.V. All rights reserved.

1. Introduction

The α-MnS manganese sulfide belongs to the MnO-type materials with strong electron correlations and the rock salt structure [1,2]. Under hydrostatic pressure, such systems exhibit a number of intriguing features, including the insulator-to-metal transition, reduction of the magnetic moment (the high-spin to low-spin transition), and the crystal symmetry transformation (see [3,4] and references therein). Below Neel temperature T_N, the MnO-type oxides and MnS sulfide exhibit the FCC-II (AFM-II) antiferromagnetic order [5,6]. Under ambient conditions, these materials are magnetic semiconductors. Under a hydrostatic pressure of 50–100 GPa at room temperature, the MnO-type compounds undergo the insulator-to-metal transition [4]. The effect of the pressure on the magnetic and crystal structures of the compounds is of great practical importance [7–9]. In pure MnS, the stepwise semiconductor-to-metal transition occurs at room temperature under a pressure of about 26 GPa [10].

In this study, we simulated the effect of the hydrostatic pressure on the physical properties of MnS with the use of the chemical pressure induced by substitution of Fe^{2+} ions (the ionic radius is 0.92 Å, high-spin octahedral state) for Mn^{2+} ions (the ionic radius is 0.97 Å, high-spin octahedral state). We synthesized new Mott-type compounds with the chemical formula $Fe_XMn_{1-X}S$ ($0 \leqslant X < 0.3$) and the rock salt structure and investigated their structural properties using single-crystal and powder neutron diffraction.

2. Experimental

Synthesis of the $Fe_XMn_{1-X}S$ single crystals and their X-ray diffraction study were described in detail in [11]. Powder neutron diffraction study of the $Fe_XMn_{1-X}S$ samples with $x = 0.05$, 0.18, and 0.27 was carried out using a D1A thermal diffractometer (Institut Laue-Langevin (ILL)) with $\lambda = 1.91$ Å at temperatures of 2–300 K. Single-crystal neutron diffraction study of the samples with $x = 0.25$ and 0.29 was carried out using a TriCS thermal instrument [12] and a SINQ neutron spallation source (Paul Scherrer Institute (PSI)) at $\lambda = 1.178$ Å in an Eulerian cradle at temperatures of 2–300 K. Simultaneously, the integral intensity and (hkl) position of magnetic and nuclear peaks were determined. The neutron and X-ray diffraction data were refined using a Fullprof program [13] based on the Rietveld method. The lattice strain was measured at the Kirensky Institute of Physics. Thermal expansion of the lattice was measured using a NETZSCH DIL-402C push rod dilatometer with a fused silica sample holder in the temperature range 120–300 K at a heating rate of 3 K min^{-1}. The results obtained were calibrated with the use of the SiO_2 reference to eliminate the influence of thermal expansion of the system. Parallelepiped samples for investigations were cut from large single crystals. Distance L between the MnS surfaces was 4.915 mm. These samples were also used for measuring the coefficient of thermal expansion of the lattice.

---

* Corresponding author.
  E-mail address: agm@iph.krasn.ru (G. Abramova).

3. Results and discussion

According to the X-ray data, at room temperature the $Fe_xMn_{1-x}S$ single crystals, similar to the α-MnS phase, have the NaCl-type face-centered cubic (FCC) structure (sp. gr. Fm-3m). Substitution of Fe^{2+} ions for Mn^{2+} ions in $Fe_xMn_{1-x}S$ decreases the lattice parameter from 5.224 ($x = 0$) to 5.165 Å ($x = 0.29$). The obtained FCC unit cell parameter of the $Fe_xMn_{1-x}S$ samples with $x = 0.29$ under chemical pressure x at 300 K (Fig. 1) is similar to the parameter of MnS under a hydrostatic pressure of 3–4 GPa [14].

The single-crystal and powder neutron diffraction data obtained on a D1A (ILL) and TriCS (PSI) at different temperatures show a similarity of the $Fe_xMn_{1-x}S$ aMnS structure. Above the Néel transition, single-crystal and powder neutron diffraction patterns contain only odd (111, 113, 331, and 511) Bragg reflections that correspond to the nuclear reflections typical of the MnS paramagnetic state (sp. gr. Fm-3m). Upon substitution of Fe ions for Mn ions in the $Fe_xMn_{1-x}S$ samples, the integral intensity of nuclear Bragg reflections from the odd planes decreases and that from the even planes increases, because manganese (-0.37) and iron ($+0.96$) ions have negative and positive neutron scattering amplitudes (in the units of 10^{-12} cm [15,16]). Since iron and sulfur ions have positive neutron scattering amplitudes, the FeO neutron diffraction pattern, in contrast to the MnS and MnO patterns, contains even planes [5,6,17,18]. Substitution of Fe^{2+} ions ($S = 2$) for Mn^{2+} ions ($S = 5/2$) in the $Fe_xMn_{1-x}S$ compounds changes the integral intensity of reflections in the patterns, which is also indicative of the $Fe_xMn_{1-x}S$ solid solution formation.

Below Neel temperature T_N, MnO, FeO, and MnS exhibit the FCC-II (AFM-II) antiferromagnetic order with ferromagnetic (FM) sheets of the (111) planes antiferromagnetically stacked along the [111] direction [5,6,17,18]. The MnO, FeO, and NiO lattices are trigonally distorted along the [111] direction. Thus, the lattice

symmetry is consistent with the magnetic structure symmetry [5,6]. The magnetic reflections caused by the AFM-II order arise at the ($h/2$ $k/2$ $l/2$) reciprocal lattice points, where h, k, and l are the odd numbers.

Fig. 2 presents D1A powder neutron diffraction patterns ($\lambda = 1.91$ Å) for $Fe_xMn_{1-x}S$ with $x = 0.05$ at 200 and 10 K. The $Fe_xMn_{1-x}S$ ($x = 0.05$) magnetic structure is similar to the MnS magnetic structure [17,18]. It was established that the direction of the magnetic moments of Mn ions in the sample corresponds to $\langle 110 \rangle$ (insert in Fig. 2b). The magnetic moments are ferromagnetically ordered in the (111) planes and antiferromagnetically ordered between these planes with the spin propagation vector (1/2,1/2,1/2).

Fig. 3 presents D1A powder neutron diffraction patterns ($\lambda = 1.911$ Å) for the $Fe_xMn_{1-x}S$ samples at 2 K. The $Fe_xMn_{1-x}S$ ($x \approx 0.1$) magnetic structure is typical of A-type antiferromagnets in the Roth classification [6]. The $Fe_xMn_{1-x}S$ ($x \approx 0.2$) magnetic structure can be presented as a B-type antiferromagnet in the Roth classification [6]. Only odd magnetic Bragg reflections are observed. The intensity of all the odd magnetic peaks with the spin propagation vector (1/2,1/2,1/2) drops to zero at T_N.

Fig. 4a presents temperature dependences of the relative integral intensity of the magnetic Bragg reflections $I(T)/I(2\ K)$ for the $Fe_xMn_{1-x}S$ samples. The integral intensity of a peak on the pattern is given by $I = Öp$ (ImaxFWHM), where FWHM is the peak full width at half maximum Magnetization M of the magnetic sublattice is proportional to the squareroot neutron intensity In $Fe_xMn_{1-x}S$, we observed the Neel temperature shift from 150 ($x = 0$) to 200 ± 3 K ($x = 0.29$) related to an increase in chemical pressure X. This indicates the enhancement of the superexchange interaction constant with decreasing distance between magnetic ions upon substitution of Fe for Mn. We estimated the exchange integrals
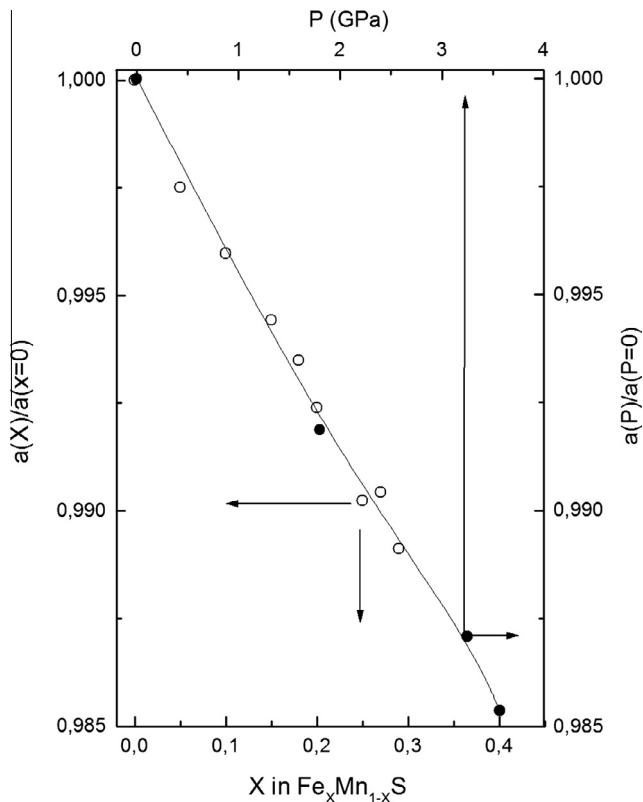

Fig. 1. Relative NaCl cubic lattice parameters of MnS under hydrostatic pressure P [14] and $Fe_xMn_{1-x}S$ upon substitution of Fe for Mn at room temperature.
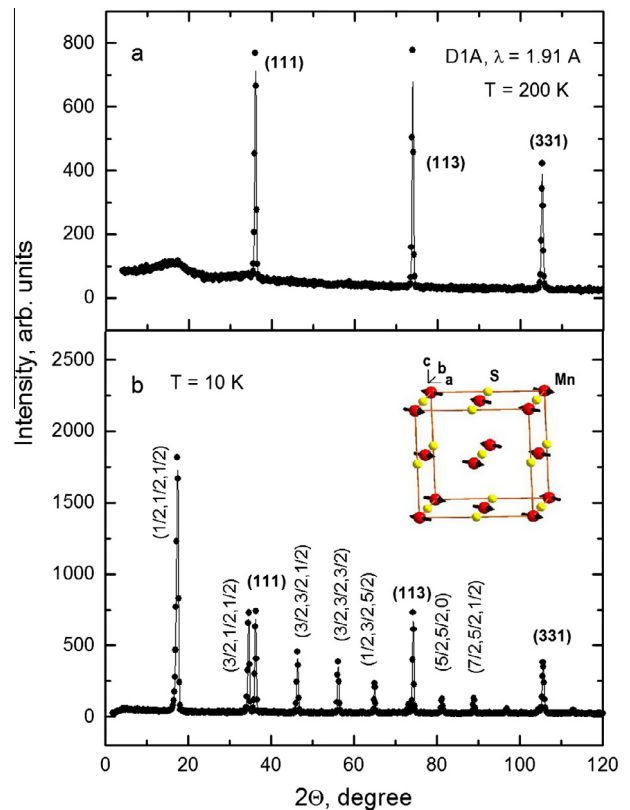

Fig. 2. Powder neutron diffraction patterns for $Fe_xMn_{1-x}S$ ($x = 0.05$) at 200 K (paramagnetic state) and 10 K (antiferromagnetic state). Insert: the Mn ion magnetic moment direction in the NaCl lattice.
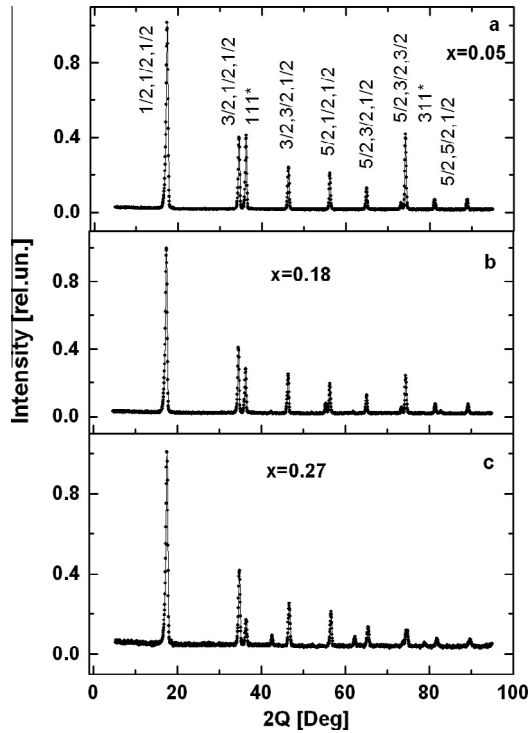
Fig. 3. Powder neutron diffraction patterns for $Fe_xMn_{1-x}S$ with x = (a) 0.05, (b) 0.18, and (c) 0.27 at 2 K.
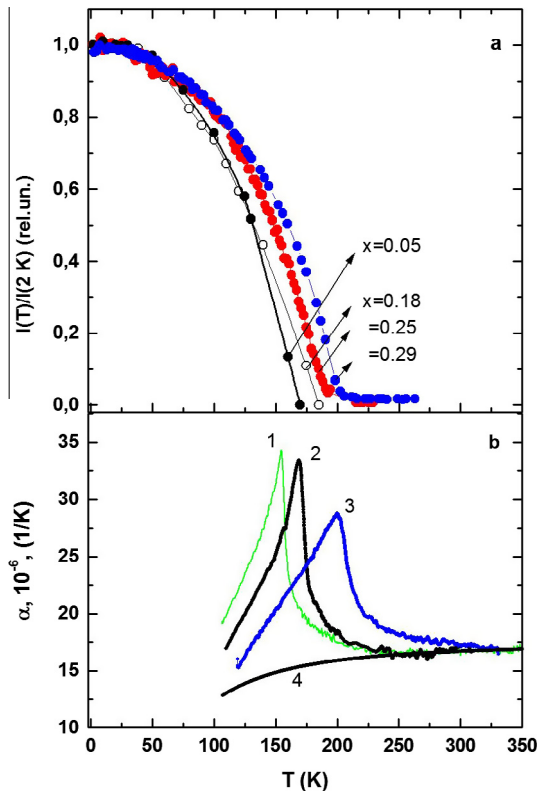

Fig. 4. Temperature dependences of the relative integral intensity of the magnetic reflections (a) and thermal expansion coefficient α (b) for $Fe_xMn_{1-x}S$ samples, b: MnS (1); x = 0.1 (2); x = 0.29 (3); without the anomalous lattice behavior (4).

using the model proposed in [19,20]; more detailed calculation data will be presented elsewhere.

The estimated exchange integral of the superexchange interaction along the $\langle 100 \rangle$ direction of the (Mn,Fe)–S–(Mn,Fe) bonds is $J^{180} = -4.15$ K for MnS and $J^{180} = -7.27$ K for $Fe_xMn_{1-x}S$ (x = 0.29).

The authors of studies [21–23] reported a minor rhombohedral distortion of the MnS NaCl-type cubic lattice at 150 and 200 K, respectively. At low temperatures (2–7 K), we observed no traces of the lattice symmetry transformation in $Fe_xMn_{1-x}S$ with $0 < x < 0.25$. However, there is an anomaly of thermal expansion coefficient α at the Neel temperature (α is measured along the [100] lattice direction, i.e., in the (100) planes). Temperature dependences of the lattice thermal expansion coefficient $\alpha = (1/L)dL/dT$ for the $Fe_xMn_{1-x}S$ single crystals are shown in Fig. 4b. In a wide temperature range (100–260 K for MnS), one can see the anomalous contribution to α, which attains its maximum at the Neel temperature.

The temperature dependence of magnetization M_{rel} (in relative units) obtained as $Imax(T) * FWHM$ $(T = 1$ K$)Imax(T = 1$ K$) * FWHM(T)$ for $Fe_xMn_{1-x}S$ (x = 0.05, T_N = 165 K) is shown in Fig. 5. For comparison, the temperature dependence of relative anomalous contribution S_{rel} to the MnS lattice strain (T_N = 150 K) is shown. The relative anomalous lattice strain is determined as $S_{rel} = dL/L_m$ $(T)/dL/L_m$ $(T = 100$ K$)$, $S_{rel} < 0$ (not shown in the figure). The temperature dependences of the structural and magnetic properties are consistent, which allows us to conclude that the anomalous contribution $dL/L_m < 0$ to the lattice strain near the Neel temperature is due to the magnetic transition (the negative magnetoelastic effect along the [100] lattice direction for MnS). Magnetoelastic constants $B1$ along the [100] direction and B2 along the [111] direction of the FCC lattice can be estimated from the anomalous contribution to the lattice strain $(dL/L)_{m\langle 100 \rangle} = -(2/3)B1/(C_{11} - C_{12})$ and $(dL/L)_{m\langle 111 \rangle} = -(2/3)B2/C_{44}$ in the magnetically ordered state, where C_{11}, C_{44}, and C_{12} [21–23] are the MnS elastic modules. The observed $(dL/L)_m$ value along the [100] direction is -0.0008 at 106 K for MnS; therefore, $(C_{11}-C_{12}) = 0.69$
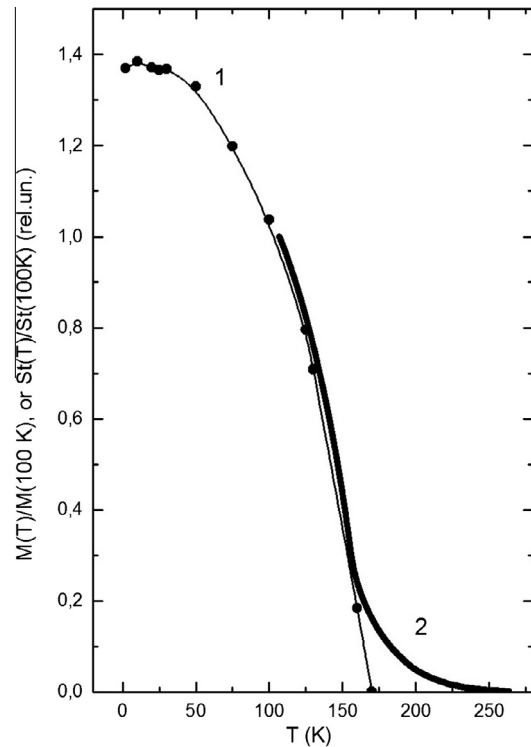

Fig. 5. Comparison of relative magnetization M_{rel} of $Fe_xMn_{1-x}S$ with x = 0.05 (curve 1) and relative anomalous lattice strain S_{rel} of MnS (curve 2, negative anomalous lattice strain).

$\times 10^{+12}$ din/cm^2. The estimated value B1 = 83 J/cm^3 for MnS at 106 K is typical of spinel compounds of 3d elements.

Thus, substitution of Fe for Mn reduces cubic lattice parameter a and enhances the Neel temperature. The MnS Neel temperature shifts caused by the substitution and hydrostatic pressure [14] are compared in Fig. 6. A linear increase in the Neel temperature with increasing X in Fe$_X$Mn$_{1-X}$S is observed only at $x < 0.25$. In the Fe$_X$Mn$_{1-X}$S samples with $0.25 < X < 0.29$, the differences from the manganese monosulfide are observed.

The magnetic properties of the Fe$_X$Mn$_{1-X}$S single crystals with $x = 0.25$ and 0.29 were investigated by a TriCS method at the PSI. Temperature dependences of the integral intensity of magnetic peaks (Fig. 7c) are similar to those for the Fe$_X$Mn$_{1-X}$S samples with $x < 0.25$. Upon heating and cooling the samples with $x = 0.25$ and 0.29, the temperature hysteresis of magnetization of about 10° at the Neel temperature is observed. This indicates the occurrence of the first-order magnetic transition. The low residual intensity of magnetic peaks is observed at $T > T_N$ in zero magnetic field and can be indicative of the short-range order at temperatures up to 220 K. We established that, in addition to the magnetic transition, the Fe$_X$Mn$_{1-X}$S single crystals with $x \geqslant 0.25$ undergo a structural phase transition at the crystal symmetry transformation. Fig. 7b presents temperature dependences of the unit cell parameters for the sample with $x = 0.25$, which are calculated from the (1 1 1) and (3 1 1) nuclear reflections. The magnetic structure can be preliminary described by the three propagation vectors: $k1 = (1/2,1/2,1/2,)$, $k2 = (1/2,1/2,0)$, and $k3 = (1/2,0,0)$. However, to make a correct conclusion, it is necessary to clarify the new nuclear lattice symmetry in these samples. The temperature evolution of the (1 1 1) reflection and lattice parameter a(1 1 1) of the NaCl phase for the sample with $x = 0.25$ (Fig. 7b) is similar to MnO at 3.3 GPa described in [22–23]. Such a behavior of the (1 1 1) reflection can be explain by splitting of this reflection into two reflections, (0 0 3) and (1 0 1), due to the structural transition from the cubic Fm-3m to rhombohedral R3m phase. The neutron
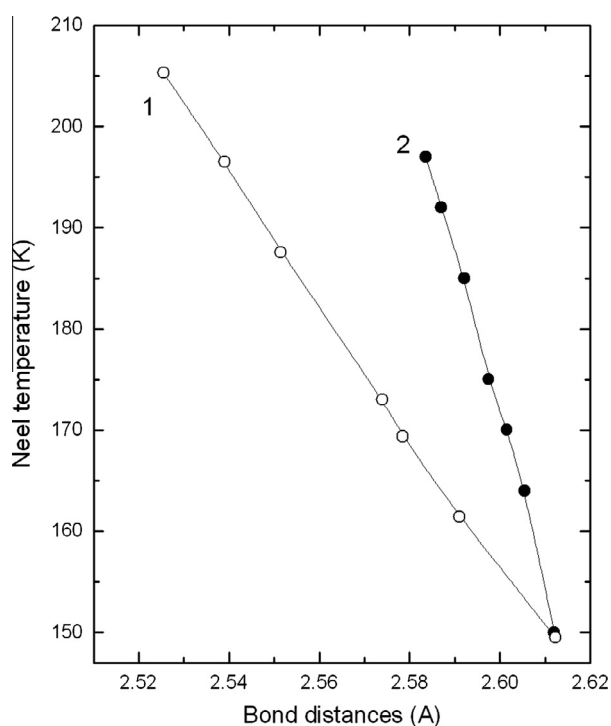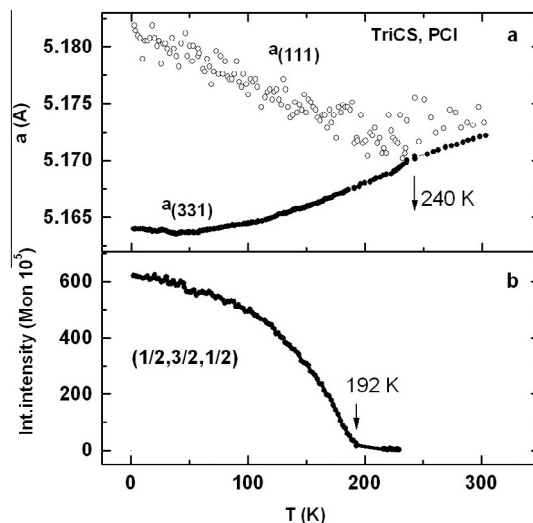

Fig. 7. Temperature dependences of the lattice parameter (a), and integral intensity of the magnetic peak (1/2,3/2,1/2) (b) for $x = 0.25$.

experiment geometry allowed us to observe only the transformation of the (1 1 1) reflection of the Fm-3m state to the (0 0 3) reflection of the R3m phase. It can be seen from Fig. 7b that the structural transition is observed at about 240 K and precedes the magnetic transition at $T_N = 192$ K. The similar situation is observed for the composition with $x = 0.29$: the structural transition is observed at about 314 K and the magnetic transition, at about 200 K. Since the critical temperatures of the structural transformation and magnetic transition in Fe$_X$Mn$_{1-X}$S are different, the observed structural transition can be of the nonmagnetic nature.

4. Conclusions

The effect of chemical pressure (cation substitution of Fe) on the magnetic and structural properties of the α-MnS manganese sulfide belonging to the MnO-type substances at temperatures of 2–300 K was investigated. It was established that the chemical pressure in the Fe$_X$Mn$_{1-X}$S compounds ($0 < x < 0.25$) upon substitution of Fe cations for Mn ions reduces the cubic lattice parameter and enhances the Neel temperature. As in MnS, the magnetic structure of Fe$_X$Mn$_{1-X}$S solid solutions at $x \approx 0.1$ is typical of A-type antiferromagnets. The magnetic structure of Fe$_X$Mn$_{1-X}$S at $x \approx 0.2$ can is typical of B-type antiferromagnets in the Roth classification. For the Fe$_X$Mn$_{1-X}$S ($0.25 < x < 0.29$), the nuclear and magnetic lattice symmetry transformation was observed.

The comparative analysis of the data presented in Figs. 1 and 5 suggests that the mechanisms of chemical and hydrostatic pressures in MnS and its solid solutions can be different, in particular, due to the occurrence of additional electrons injected by an iron ion in the MnS matrix.

Fig. 6. Neel temperature vs bond distances for (1) MnS and (2) Fe$_X$Mn$_{1-X}$S. Comparison of the Neel temperature shifts in MnS under hydrostatic pressure [14] and upon substitution of Fe (our investigation).

References

[1] N.F. Mott, E.A. Devis, Phill. Mag. 17 (1968) 1269.
[2] V.I. Anisimov, J. Zaanen, O.K. Andersen, Phys. Rev. B 44 (1991) 943.
[3] D. Kasinathan et al., Phys. Rev. B 74 (2006) 195110.
[4] R.E. Cohen, I.I. Mazin, D.G. Isaak, Science 275 (1997) 654.
[5] M.E. Lines, E.D. Jones, Phys. Rev. 141 (2) (1966) 525.
[6] W.L. Roth, Phys. Rev. 110 (6) (1958) 1333.
[7] Z. Fang, I.V. Solovyev, H. Sawada, K. Terakura, Phys. Rev. B 59 (1999) 762.
[8] T. Kondo, T. Yagi, Y. Syono, Y. Noguchi, T. Atou, T. Kikegawa, O. Shimomura, J. Appl. Phys. 87 (2000) 4153.
[9] Y. Ding et al., Phys. Rev. B 74 (2006) 144101.
[10] Y. Mita, M. Kobayashi, S. Endo, S. Mochizuki, J. Mag. Magn. Mat. 272–276 (2004) 428.
[11] G. Abramova, N. Volkov, G. Petrakovskiy, et al., J. Mag. Magn. Mater. 320 (2008) 3261. + messba.
[12] J. Schefer, M. Boehm, L. Keller, et al., Physica B 283 (2000) 302.
[13] J. Rodriguez-Carvajal, Physica B 192 (1993) 55.
[14] C.A. McCammon, Phys. Chem. Min. 17 (1991) 636.
[15] V.F. Sears, Neutron News 3 (1992).
[16] S.W. Lovesey, Theory of Neutron Scattering from Condensed Matter, Clarendon Press, Oxford, 1987.
[17] L.M. Corliss, N. Elliott, J.M. Hastings, Phys. Rev. 104 (1956) 924.
[18] J.S. Sweeney, D.L. Heinz, Phys. Chem. Min. 22 (1993) 63.
[19] M.V. Eremin, The theory of the exchange interaction of the magnetic ions in dielectrics. Spectroscopy of Crystals (L., Science, 1985).
[20] O.A. Bajukov, A.F. Sawicki, Fiz. Tverd. Tela (Russian) 36 (1994) 1923.
[21] B. Morosin, Phys. Rev. B 1 (1970) 236.
[22] H. van der Heide, C.F. van Bruggen, G.A. Wiegers, C. Haas, J. Phys. C: Solid State Phys. 16 (1983) 855.
[23] A.P. Kantor, L.S. Dubrovinsky, N.A. Dubrovinskaia, I.Yu. Kantor, I.N. Goncharenko, J. Alloys Comp. 402 (2005) 42 (III).